Available online at www.sciencedirect.com

ScienceDirect

Procedia Engineering 10 (2011) 1451–1456

Engineering Procedia

ICM11

Effect of Internal Pressure on Tensile Strain Capacity of X80 Pipeline

Satoshi Igi*, Takahiro Sakimoto, Shigeru Endo

JFE Steel Corporation, 1 Kawasaki, Chuo, Chiba 260-0835, Japan

Abstract

This paper examines the influence of internal pressure on the tensile strain capacity of pipelines. A pressurized full-pipe tension test and curved wide plate (CWP) test were conducted together with FE analyses in order to investigate the strain behavior of pipe under large axial loading with high internal pressure. The critical tensile strain drastically decreased under a high internal pressure condition. Single edge notch tension (SENT) tests with shallow notched specimens were also performed to obtain the material resistance curve (R-curve), and a series of FE analyses was conducted to obtain the crack driving force for ductile crack propagation. The R-curve and crack driving force curve were used in predicting the tensile strain limit of X80 girth welded pipe with a surface defect in the HAZ. The predicted critical tensile strain showed good agreement with that obtained in the pressurized full-pipe tension test. These results demonstrate that the tensile strain capacity of pressurized pipes can be predicted by using the R-curve from SENT tests and the crack driving force curve from FE analyses.

Keywords: X80 linepipe; Internal pressure; Tearing resistance; Pipe tension test; CWP test; SENT test; R-curve

1. Introduction

In recent years, construction of natural gas pipelines has expanded into severe environments, such as seismic and permafrost regions. High-strength linepipes such as X80 and X100 grade are being developed continuously in order to improve transportation efficiency and reduce construction costs [1]. It can be assumed that pipelines in the above-mentioned environments will be subjected to large deformation due to ground movement associated with liquefaction in seismic regions and frost heave in permafrost regions. It is not possible to apply conventional stress-based design or integrity assessment methods when a pipeline is subjected to large plastic strain that greatly exceeds the yield stress of the pipe material. The most critical fracture mode in pipelines is considered to be ductile fracture initiated and propagated from defects in girth welds. The tensile strain capacity of a pipeline is usually characterized using uniaxial tests

* Corresponding author. Tel.: +81-43-262-2420; fax: +81-43-262-2117.
E-mail address: s-igi@jfe-steel.co.jp.

such as curved wide plate (CWP) tests [2, 3]. However, CWP tests cannot consider the effect of internal pressure in strain capacity evaluations. Therefore, it is important to investigate of the effect of internal pressure on ductile fracture behavior. Full-scale pressurized and un-pressurized tensile tests using X65 ERW pipe and welds have been conducted to investigate the influence of internal pressure on the tensile strain capacity of pipelines [4]. These tests indicated that internal pressure does not seem to affect the ductile tearing resistance curve. However, the influence of internal pressure on ductile crack growth behaviors is not fully understood, as only limited data are available due to the difficulty of performing pressurized pipe tension tests, especially for high-strength linepipes such as API X80 grade.

Given these circumstances, in this research, the influence of internal pressure on ductile tearing behaviors and tensile strain capacity was investigated by conducting pressurized full-pipe tension tests using pipe specimens with artificial surface notches. FE analysis was also conducted to clarify the strain behavior of the pressurized pipe under large axial loading. A SENT test with a shallow notch specimen was performed to obtain the material resistance curve for ductile cracking, and a series of FE analyses was conducted to obtain the crack driving force for ductile crack propagation. The R-curve and crack driving force curve were then used to predict the tensile strain limit of X80 girth welded pipe with a surface defect in the heat affected zone (HAZ).

2. Experimental procedure

2.1. Tested material

The test specimens were taken from API 5L X80 linepipes with an outside diameter (OD) of 508mm and wall thickness (WT) of 14.3mm. The typical tensile properties of the tested materials are shown in Table 1. The stress–strain (S-S) curve of the base material of the tested X80 linepipe shows roundhouse-type work hardening characteristics, in which yield elongation is not observed. Both the yield stress and the tensile strength of the welded metal show higher strength than those of the base metal, and the WM shows perfectly overmatched tensile properties. Girth welded joints of the X80 linepipe were produced by gas metal arc welding (GMAW). The GMAW conditions are summarized in Table 2, which also shows a macroscopic photograph of the joint cross section.

2.2. Tension test

The dimensions and geometry of the full-pipe tension test specimen are shown in Fig. 1. Two artificial surface notches (70mm in length, 3.0mm in depth and 50mm in length, 3.0mm in depth) were introduced by electrical discharge machining (EDM) in the HAZ of the girth welded joint on the outer pipe surface. A full-pipe tension test was conducted under constant internal pressure, and the corresponding hoop stress was equivalent to 72% of the specified minimum yield strength. The dimensions and geometry of the CWP test specimen are shown in Fig. 2. A CWP test was conducted in order to verify the tensile capacity under a condition of no internal pressure. During the tension tests, the load, crack mouth opening displacement (CMOD), and axial elongation were recorded using a load cell, clip gauge, and LVDT, respectively. After the tests, microscopic sectional observation was performed to measure the propagating ductile crack length and the amount of notch tip displacement.

SENT specimens were taken from the pipe body, as illustrated in Fig. 3. An edge notch was also introduced by EDM. Simulated girth welding heat cycles were applied to the specimens before notch machining. The peak heating temperatures of the simulated HAZ were 1400°C (coarse grained region) and 900°C (fine grained region). Rapid heating was performed for 6sec to these peak temperatures using a Gleeble tester, followed by rapid cooling by nitrogen gas without holding time. Because the actual cooling time from 800°C to 500°C was 15sec, the equivalent heat input was 1.7kJ/mm in GMAW. The SENT tests were unloaded at the specific CMOD to investigate ductile crack propagation behaviors.

Microscopic sectional observation was performed to measure the propagating ductile crack length and amount of notch tip displacement, as illustrated in Fig. 4. The effective opening displacement, δ_{eff}, is defined as the displacement between the intersections of the notch shape and extended lines pulled with an angle of 90° from the notch tip.

Table 1. Tensile property in longitudinal direction

X80 grade	YS [MPa]	TS [MPa]	uEL [%]
Base metal	551	679	8.4
Weld metal	603	773	-

Table 2. Welding conditions

Welding consumable	KOBELCO MGS-70
Shielding gas	80%Ar-20%CO_2
Current-Voltage-Speed	180A-18V-180mm/min
Heat input	10.8 kJ/cm
Preheating	Not applied
Welding machine	MAX-II(JFE Eng. Corp.)
Macrostructure	

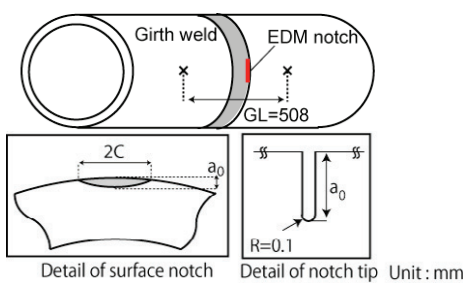

Fig. 1. Pipe specimen with two surface notches

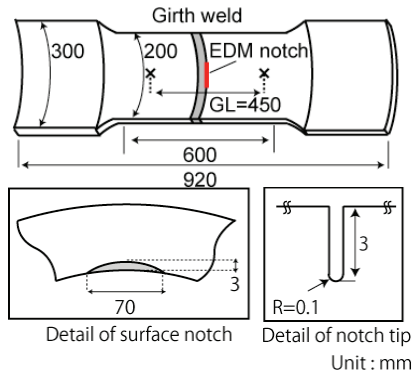

Fig. 2. CWP specimen with surface notch

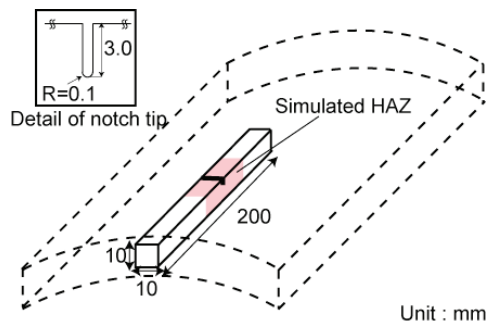

Fig. 3. Geometry and size of SENT specimen

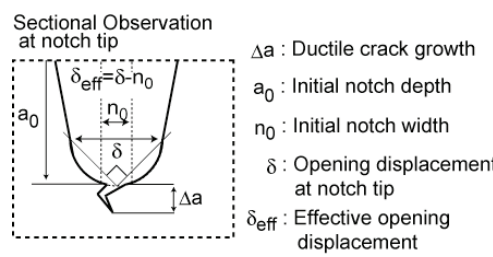

Fig. 4. Definition of effective opening displacement

2.3. Finite element analysis procedure

In order to investigate the crack driving force during ductile crack propagation in the pipe specimen, 3-dimensional finite element (FE) analyses were performed using 1/4 symmetrical models with the commercial code ABAQUS 6.7. The initial notch geometry included in the tests was reproduced exactly in the models. The minimum element size at the notch tip was 0.025mm x 0.025mm x 0.5mm. FE models with various notch depths were prepared to represent the increasing notch depth during ductile tearing. The relationship between the effective opening displacement and global strain was obtained from the

FEA results. This global strain is defined as the tensile strain calculated from the elongation between the same points in the full-pipe test.

3. Experimental results and discussion

3.1. Crack resistance curves for X80 linepipe

Full-scale pipe tension tests and SENT tests using seamless pipe were performed to investigate the influence of internal pressure and specimen geometry on the R-curves [5]. The R-curves of pressurized and non-pressurized pipes and the SENT tests show good coincidence. These results indicate that the R-curve obtained from SENT tests is applicable as the curve for a pressurized pipe. As representative examples of ductile crack propagation behavior at the notch tip, Fig. 5 shows the results of microscopic sectional observation of the SENT tests specimens of a base material of X80 and simulated HAZ (maximum heating temperature: 1400ºC). It can be recognized that a ductile crack has propagated from the deepest point of the notch tip in the thickness direction. Figure 6 shows the relationship between δ_{eff} and the ductile crack length for the base material and simulated HAZ. The R-curves for the base material coincide almost exactly with that for the simulated HAZ.

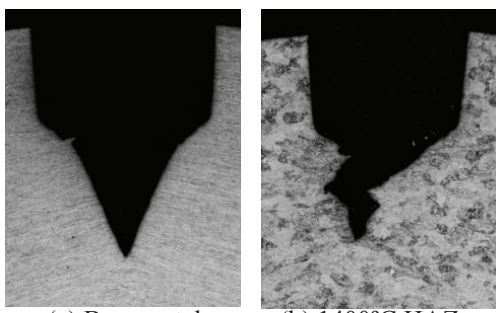

(a) Base metal (b) 1400ºC HAZ

Fig. 5. Comparison of ductile crack propagation behavior

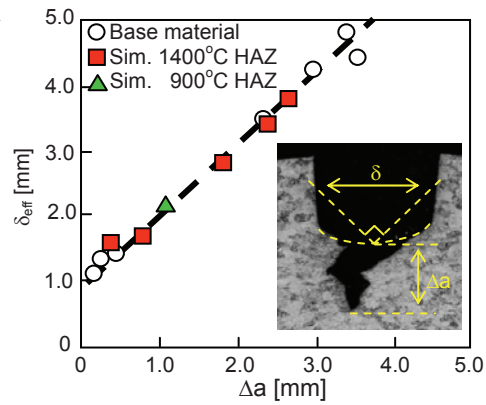

Fig. 6. R-curve of base material and simulated HAZ

3.2. Effect of internal pressure on tensile strain capacity

A comparison of the nominal stress versus global strain relationships in the full-pipe tension test and CWP tests is shown in Fig. 7. Due to the end cap effect, the nominal stress calculated from the actual applied load in the pressurized pipe test is lower than that in the CWP test. However, almost the same nominal stresses were observed after the end cap effect was corrected. A significant decrease of approximately 50% is observed in the tensile strain capacity in the pressurized pipe test compared to the CWP test. Figure 8 shows the CMOD versus global strain relationships for the pipe and CWP tests. In the pressurized pipe test, CMOD increases beyond 2% global strain. In contrast, CMOD drastically increased to beyond 4.5% global strain in the CWP test. These results indicate that the crack driving force of a HAZ defect increases under high internal pressure conditions. Figure 9 shows the effect of internal pressure on the hoop strain and radial strain (thickness direction) under the same longitudinal tensile strain of 2% calculated by FE analyses. Under a condition of no internal pressure, the hoop strain and radial strain obey the law of conservation of volume with respect to plasticity, and show the same strain value. Because the decrease in the pipe diameter becomes smaller as the internal pressure increases, hoop strain also shows similar changes corresponding to the change in pipe diameter accompanying changes in internal pressure. The negative strain value in the radial direction increases as internal pressure increases,

and the crack driving force of a surface notch increases under high internal pressure conditions. As a result, the strain capacity may decrease under a high internal pressure condition.

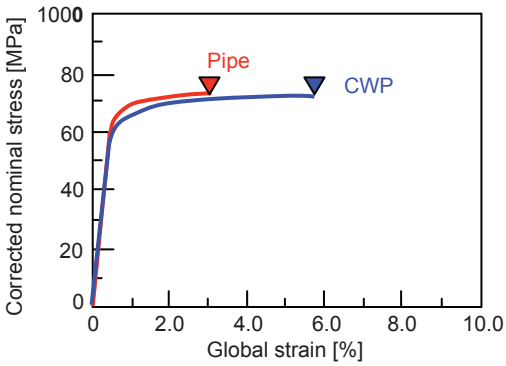

Fig. 7. Nominal stress versus global strain relations

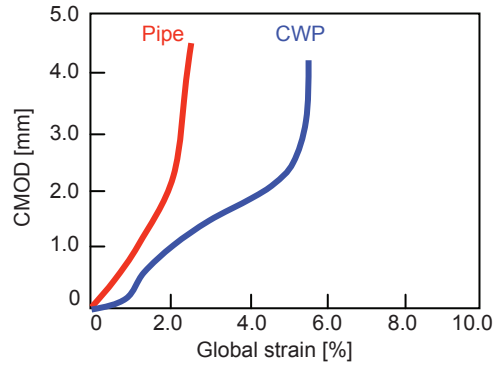

Fig. 8. CMOD versus global strain relations

3.3. Tensile strain capacity prediction for pressurized pipe test

Figure 10 shows the results of sectional observation of the notch region after Nital etching. A ductile crack propagated through the HAZ toward the maximum shear stress direction, which was inclined about 45° to the loading axis. The R-curve from the SENT test may be applicable as the curve of a pressurized girth welded pipe when a ductile crack initiates from a surface notch and propagates through the HAZ or base metal. This indicates that the tensile strain capacity of pressurized pipes can be predicted using the R-curve obtained by SENT tests when the crack driving force curve is also available for the ductile tearing analysis. The prediction procedure for the tensile strain limit is summarized in the following four steps, as shown in Fig. 11. In the first step, the R-curve is obtained experimentally by SENT tests for the base material. In the second step, the relationship of δ_{eff} vs. global strain of the pipe is calculated by FEA using a series of FE models with increasing notch depths. In the third step, a new crack driving force curve for a propagating crack is obtained by connecting the same δ_{eff} in the R-curve and the crack driving force curves for stationary cracks through equal levels of crack propagating length, Δa. In the last step, tensile strain capacity is predicted at the point where δ_{eff} increases drastically. The tensile strain capacity obtained by this procedure is compared with that in the full-pipe tension test in Fig. 12. Although the predicted tensile strain is slightly lower than that in the full-pipe tension test, predicted strain is substantially in good agreement. These results indicate that the tensile strain capacity of pressurized pipes can be predicted by using the R-curve from SENT tests and the crack driving force curve from FE analyses.

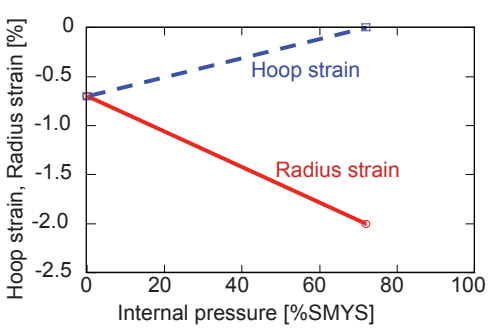

Fig. 9. Effect of internal pressure on strains

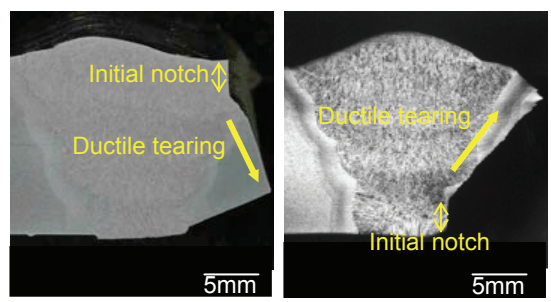

(a) Pipe test (b) CWP test

Fig. 10. Ductile tearing from initial notch

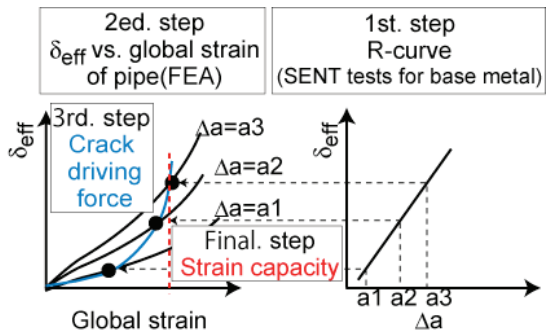

Fig. 11. Schematic chart of prediction procedure

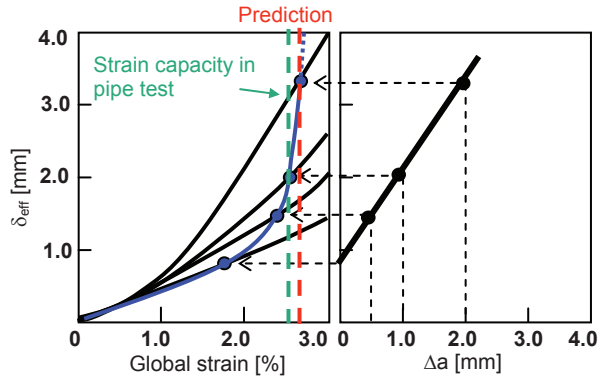

Fig. 12. Prediction results of tensile strain capacity of pressurized pipe specimen

4. Conclusions

The influence of internal pressure on strain capacity was investigated by conducting a full-pipe tension test and CWP test. A prediction procedure for tensile strain capacity was also developed by conducting SENT tests and FE analyses. The following conclusions were obtained.

1. The R-curve for the base material coincides almost exactly with that for the simulated HAZ. The SENT test is useful in predicting the R-curves of a pressurized pipe with a surface notch when a ductile crack from a surface notch propagates in the HAZ and/or base material.
2. The negative strain value in the radius direction increases as internal pressure increases, and the crack driving force of a surface notch increases under high internal pressure conditions.
3. The tensile strain capacity of pressurized pipes can be predicted by using the R-curve from SENT tests and the crack driving force curve from FE analyses. Predicted critical strain shows good agreement with the strain at leakage in full-pipe tension test.

References

[1] Glover, A., Zhou, J., Horsley, D., Suzuki, N., Endo, E., and Takehara, J. (2003); "Design, Application and Installation of an X100 Pipeline," Proc. of 22nd International Conference on Offshore Mechanics and Arctic Engineering, OMAE2003-37429

[2] Denys, R., De Waele, W., Lefevre, A. and De Baets, P. (2004); "An Engineering Approach to the Prediction of the Tolerable Defect Size for Strain-Based Design," Proc. of 4th International Conference on Pipeline Tech, Ostend, pp.163-181

[3] Igi, S., Suzuki, N. (2007); "Tensile Strain Limits of X80 High-strain Pipelines" Proc. of 17th International Offshore and Polar Engineering Conference

[4] Gioielli, P. C., Minnaar, K., Macia, M. L., Kan, W. C. (2007) "Large-Scale Testing Methodology to Measure the Influence of Pressure on Tensile Strain Capacity of a Pipeline" Proc. of 17th International Offshore and Polar Engineering Conference

[5] Sakimoto, T., Igi, S., Kubo, T., Ohata, M., Minami, F. (2009); "The Influence of Internal Pressure on Ductile Fracture Behavior from a Surface Defect on a Pipe," Proc. of 19th International Offshore and Polar Engineering Conference, Osaka.